Meccanica (2006) 41:661–670
DOI 10.1007/s11012-006-9012-z

Flapwise bending vibration analysis of double tapered rotating Euler–Bernoulli beam by using the differential transform method

Ozge Ozdemir Ozgumus · Metin O. Kaya

Received: 12 November 2005 / Accepted: 27 February 2006 / Published online: 31 October 2006

Abstract In this study, the out-of-plane free vibration analysis of a double tapered Euler–Bernoulli beam, mounted on the periphery of a rotating rigid hub is performed. An efficient and easy mathematical technique called the Differential Transform Method (DTM) is used to solve the governing differential equation of motion. Parameters for the hub radius, rotational speed and taper ratios are incorporated into the equation of motion in order to investigate their effects on the natural frequencies. Calculated results are tabulated in several tables and figures and are compared with the results of the studies in open literature where a very good agreement is observed.

Keywords Differential Transform Method · Tapered Euler beam · Nonuniform Euler beam · Mechanics of solids and structures

1 Introduction

The dynamic characteristics, i.e., natural frequencies and related mode shapes, of rotating tapered beams are very important for the design and performance evaluation in several engineering applications including rotating machinery, helicopter blades, windmills, robot manipulators and spinning space structures because they are required to determine resonant responses and to perform forced vibration analysis. As a result, rotating tapered beams have been the subject of interest for many investigators.

This study is an extension of the authors' previous work [1]. Parameters for the hub radius, rotational speed and taper ratios are incorporated into the equation of motion in order to investigate their effects on the natural frequencies. After solving the problem by DTM, calculated results that can be used as reference values for the future studies are tabulated in several tables and figures.

The superiority of DTM over other methods is its simplicity and accuracy in calculating the natural frequencies and plotting the mode shapes and also, the variety of the problems to which it may be applied. Zhou [2] introduced the concept of this method by using it to solve both linear and nonlinear initial value problems in electric circuit analysis. Since the method can deal with nonlinear problems, Chiou and Tzeng [3] applied the Taylor transform to solve nonlinear vibration problems. Additionally, the method may be used to solve both ordinary and partial differential equations so Jang et al. [4] applied the two-dimensional differential transform method to the solution of partial differential equations. Abdel and Hassan [5] adopted the method to solve some eigenvalue problems. Since previous studies have shown that DTM is an

O. Ozdemir Ozgumus · M. O. Kaya (✉)
Istanbul Technical University, Faculty of Aeronautics and Astronautics, 34469, Maslak, Istanbul, Turkey
e-mail: kayam@itu.edu.tr

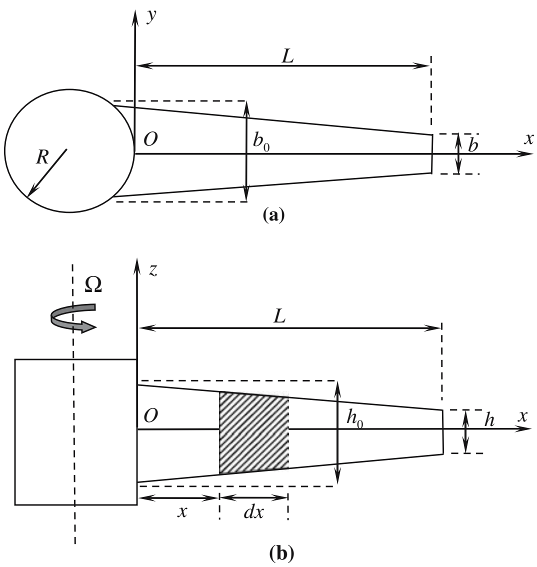

Fig. 1 (**a**) Top view (**b**) Side view of a rotating double tapered Euler–Bernoulli beam

efficient tool to solve nonlinear or parameter varying systems, recently it has gained much attention by several researchers Chen and Ju [6], Arikoglu and Ozkol [7], and Bert and Zeng [8].

2 Formulation

The governing partial differential equation of motion is derived for the out-of-plane free vibration of a rotating tapered cantilever Euler–Bernoulli beam represented by Fig. 1. Here, the cantilever beam of length L is fixed at point O to a rigid hub with radius R and it is rotating at a constant angular velocity, Ω. The beam tapers linearly from a height h_0 at the root to h at the free end in the xz plane and from a breadth b_0 to b in the xy plane. The height taper ratio, c_h and the breadth taper ratio, c_b, whose descriptions are going to be given in the following sections must be $c_h < 1$ and $c_b < 1$ because otherwise the beam tapers to zero between its ends. In the right-handed Cartesian co-ordinate system, the x-axis coincides with the neutral axis of the beam in the undeflected position, the z-axis is parallel to the axis of rotation (but not coincident) and the y-axis lies in the plane of rotation. Therefore, the principal axes of the beam cross-section are parallel to y and z directions, respectively.

The following assumptions are made in this study,

a. The out-of-plane displacement of the beam is small.
b. The cross-sections that are initially perpendicular to the neutral axis of the beam remain plane and are perpendicular to the neutral axis during bending.
c. The beam material is homogeneous and isotropic.
d. Coriolis effects are not included.

Moreover, the beam considered here have doubly symmetric cross-sections such that the shear center and the centroid of each cross-section are coincident. Therefore, there is no coupling between bending vibrations and torsional vibration.

2.1 Governing differential equations of motion

According to the Euler–Bernoulli beam theory, the governing differential equation of motion for the out-of-plane bending motion is as follows

$$\rho A \frac{\partial^2 w}{\partial t^2} + \frac{\partial^2}{\partial x^2}\left(EI_y \frac{\partial^2 w}{\partial x^2}\right) - \frac{\partial}{\partial x}\left(T\frac{\partial w}{\partial x}\right) = p_w \quad (1)$$

where w is the out-of-plane bending displacement, EI_y is the bending rigidity, ρA is the mass per unit length, T is the centrifugal force, p_w is the applied force per unit length in the flapwise direction, x is the spanwise position and t is the time. Since free vibration is considered in this study, p_w is taken to be zero.

The centrifugal force, T, that varies along the spanwise direction of the beam is given by

$$T(x) = \int_x^L \rho A \Omega^2 (R + x)\mathrm{d}x. \quad (2)$$

The boundary conditions for a cantilever Euler–Bernoulli beam can be expressed as follows

$$w = \frac{\partial w}{\partial x} = 0 \quad \text{at } x = 0 \quad (3)$$

$$\frac{\partial^2 w}{\partial x^2} = \frac{\partial^3 w}{\partial x^3} = 0 \quad \text{at } x = L. \quad (4)$$

A sinusoidal variation of $w(x,t)$ with a circular natural frequency ω is assumed and the displacement function is approximated as

$$w\,(x,t) = \bar{w}\,(x)\,\mathrm{e}^{i\omega t} \quad (5)$$

Substituting Eq. (5) into Eq. (1), the equation of motion can be rewritten as follows

$$-\omega^2 \rho A \bar{w} + \frac{\mathrm{d}^2}{\mathrm{d}x^2}\left(EI_y \frac{\mathrm{d}^2 \bar{w}}{\mathrm{d}x^2}\right) - \frac{\mathrm{d}}{\mathrm{d}x}\left(T \frac{\mathrm{d}\bar{w}}{\mathrm{d}x}\right) = 0. \tag{6}$$

2.2 Tapered beam formulation and dimensionless parameters

The general equations for the breadth $b(x)$, the height $h(x)$, the cross-sectional area, $A(x)$ and the second moment of area, $I_y(x)$ of a beam that tapers in two planes are given by

$$b(x) = b_0 \left(1 - c_b \frac{x}{L}\right)^m \tag{7a}$$

$$h(x) = h_0 \left(1 - c_h \frac{x}{L}\right)^n \tag{7b}$$

$$A(x) = A_0 \left(1 - c_b \frac{x}{L}\right)^m \left(1 - c_h \frac{x}{L}\right)^n \tag{7c}$$

$$I_y(x) = I_{y0} \left(1 - c_b \frac{x}{L}\right)^m \left(1 - c_h \frac{x}{L}\right)^{3n}. \tag{7d}$$

Here the breadth taper ratio, c_b and the height taper ratio, c_h can be given by

$$c_b = 1 - \frac{b}{b_0} \tag{8a}$$

$$c_h = 1 - \frac{h}{h_0}. \tag{8b}$$

Knowing that the subscript $()_o$ denotes the values at the root of the beam, the following formulas can be introduced.

$$A_0 = b_0 h_0 \tag{9a}$$

$$I_{y0} = \frac{b_0 h_0^3}{12}. \tag{9b}$$

Values of $n = 1$ and $m = 1$ are used in this study to model the beam that tapers linearly in two planes. Young's modulus E and density of the material, ρ are assumed to be constant so that the mass per unit length ρA and the bending rigidity EI_y vary according to the Eqs. (7c)–(7d).

The dimensionless parameters that are used to make comparisons with the studies in open literature can be given as follows [9]

$$\xi = \frac{x}{L}, \quad \delta = \frac{R}{L}, \quad \tilde{w}(\xi) = \frac{\bar{w}}{L}, \quad \eta^2 = \frac{\rho A_0 L^4 \Omega^2}{EI_{y0}}, \quad \mu^2 = \frac{\rho A_0 L^4 \omega^2}{EI_{y0}}. \tag{10}$$

Here δ is the hub radius parameter, η is the rotational speed parameter, μ is the frequency parameter, ξ is the dimensionless distance and $\tilde{w}$ is the dimensionless flapwise deformation.

Using the first two dimensionless parameters and Eq. (7c), the dimensionless expression for the centrifugal force can be given by

$$T(\xi) = \rho A_0 \Omega^2 L^2 \Big[\frac{c_b c_h}{4} + \delta - \frac{1}{2}(c_b\delta + c_h\delta - 1) - \frac{1}{3}(c_b + c_h\delta - c_b c_h \delta) - \xi\delta + \frac{\xi^2}{2}(c_b\delta + c_h\delta - 1) + \frac{\xi^3}{3}(c_b + c_h\delta - c_b c_h\delta) - \frac{\xi^4}{4} c_b c_h\Big] \tag{11}$$

Substituting tapered beam formulas, dimensionless parameters and Eq. (11) into Eq. (6), the following dimensionless equation of motion is obtained for the linear taper case ($m = 1, n = 1$).

$$\frac{\mathrm{d}^2}{\mathrm{d}\xi^2}\left[(1 - c_b\xi)(1 - c_h\xi)^3 \frac{\mathrm{d}^2\tilde{w}}{\mathrm{d}\xi^2}\right] - \mu^2 (1 - c_b\xi)(1 - c_h\xi)\tilde{w} - \eta^2 \frac{\mathrm{d}}{\mathrm{d}\xi}\Big\{\Big[\frac{c_b c_h}{4}\left(1 - \xi^4\right) + \delta(1 - \xi) + \frac{1}{2}(1 - c_b\delta - c_h\delta)\left(1 - \xi^2\right) + \frac{1}{3}(-c_b - c_h + c_b c_h \delta)\left(1 - \xi^3\right)\Big]\frac{\mathrm{d}\tilde{w}}{\mathrm{d}\xi}\Big\} = 0. \tag{12}$$

Additionally, the dimensionless boundary conditions can be expressed as follows

$$\tilde{w} = \frac{\mathrm{d}\tilde{w}}{\mathrm{d}\xi} = 0 \quad \text{at} \quad \xi = 0 \tag{13}$$

$$\frac{\mathrm{d}^2\tilde{w}}{\mathrm{d}\xi^2} = \frac{\mathrm{d}^3\tilde{w}}{\mathrm{d}\xi^3} = 0 \quad \text{at} \quad \xi = 1. \tag{14}$$

3 The Differential transform method

The Differential Transform Method is a transformation technique based on the Taylor series expansion and it is a useful tool to obtain analytical solutions of the differential equations. In this method, certain transformation rules are applied and the governing differential equations

Table 1 DTM teorems for the equations of motion

Original function	Transformed functions
$f(x) = g(x) \pm h(x)$	$F[k] = G[k] \pm H[k]$
$f(x) = \lambda g(x)$	$F[k] = \lambda G[k]$
$f(x) = g(x)h(x)$	$F[k] = \sum_{l=0}^{k} G[k-l]H[l]$
$f(x) = \frac{d^n g(x)}{dx^n}$	$F[k] = \frac{(k+n)!}{k!} G[k+n]$
$f(x) = x^n$	$F[k] = \delta(k-n) = \begin{cases} 0 & if\ k \neq n \\ 1 & if\ k = n \end{cases}$

Table 2 DTM teorems for boundary conditions

$x = 0$		$x = 1$	
Original B.C.	Transformed B.C.	Original B.C.	Transformed B.C.
$\partial/f(0) = 0$	$F[0] = 0$	$f(1) = 0$	$\sum_{k=0}^{\infty} F[k] = 0$
$\frac{df}{dx}(0) = 0$	$F[1] = 0$	$\frac{df}{dx}(1) = 0$	$\sum_{k=0}^{\infty} kF[k] = 0$
$\frac{d^2f}{dx^2}(0) = 0$	$F[2] = 0$	$\frac{d^2f}{dx^2}(1) = 0$	$\sum_{k=0}^{\infty} k(k-1)F[k] = 0$
$\frac{d^3f}{dx^3}(0) = 0$	$F[3] = 0$	$\frac{d^3f}{dx^3}(1) = 0$	$\sum_{k=0}^{\infty} k(k-1)(k-2)F[k] = 0$

and the boundary conditions of the system are transformed into a set of algebraic equations in terms of the differential transforms of the original functions and the solution of these algebraic equations gives the desired solution of the problem with great accuracy. It is different from high-order Taylor series method because Taylor series method requires symbolic computation of the necessary derivatives of the data functions and is expensive for large orders.

Consider a function $f(x)$ which is analytic in a domain D and let $x = x_0$ represent any point in D. The function $f(x)$ is then represented by a power series whose center is located at x_0. The differential transform of the function $f(x)$ is given by

$$F[k] = \frac{1}{k!}\left(\frac{d^k f(x)}{dx^k}\right)_{x=x_0} \tag{15}$$

where $f(x)$ is the original function and $F[k]$ is the transformed function.

The inverse transformation is defined as

$$f(x) = \sum_{k=0}^{\infty} (x - x_0)^k F[k] \tag{16}$$

Combining Eqs. (15) and (16), we get

$$f(x) = \sum_{k=0}^{\infty} \frac{(x - x_0)^k}{k!}\left(\frac{d^k f(x)}{dx^k}\right)_{x=x_0}. \tag{17}$$

Considering Eq. (17), it is noticed that the concept of differential transform is derived from Taylor series expansion. However, the method does not evaluate the derivatives symbolically.

In actual applications, the function $f(x)$ is expressed by a finite series and Eq. (17) can be rewritten as follows

$$f(x) = \sum_{k=0}^{q} \frac{(x - x_0)^k}{k!}\left(\frac{d^k f(x)}{dx^k}\right)_{x=x_0} \tag{18}$$

which means that $f(x) = \sum_{k=q+1}^{\infty} \frac{(x-x_0)^k}{k!}\left(\frac{d^k f(x)}{dx^k}\right)_{x=x_0}$ is negligibly small. Here, the value of q depends on the convergence rate of the natural frequencies.

Theorems that are frequently used in the transformation of the differential equations and the boundary conditions are introduced in Tables 1 and 2, respectively.

Table 3 Variation of the natural frequencies of a nonrotating Euler–Bernoulli beam with different combinations of breadth and height taper ratios ($\delta = 0$)

c_h	c_b 0	0.1	0.2	0.3	0.4	0.5	0.6	0.7	0.8
	(a) Fundamental natural frequency								
0	3.51602	3.63103	3.76286	3.91603	4.09698	4.31517	4.58531	4.93164	5.39759
	3.51602[a]	–	–	3.91603[a]	–	–	4.58531[a]	–	5.39759[a]
0.1	3.55870	3.67370	3.80552	3.95870	4.13966	4.35792	4.62822	4.97489	5.44156
0.2	3.60828	3.72328	3.85512	4.00831	4.18932	4.40768	4.67816	5.02520	5.49266
0.3	3.66675	3.78180	3.91368	4.06693	4.24802	4.46651	4.73721	5.08468	5.55297
	3.66675[a]	–	–	4.06693[a]	–	–	4.73721[a]	–	5.55297[a]
0.4	3.73708	3.85222	3.98419	4.13755	4.31878	4.53744	4.80842	5.15636	5.62552
0.5	3.82379	3.93909	4.07124	4.22480	4.40623	4.62515	4.89647	5.24492	5.71495
0.6	3.93428	4.04988	4.18235	4.33622	4.51799	4.73728	5.00903	5.35802	5.82882
	3.93428[a]	–	–	4.33622[a]	–	–	5.00903[a]	–	5.82882[a]
0.7	4.08171	4.19786	4.33086	4.48529	4.66762	4.88746	5.15976	5.50926	5.98047
0.8	4.29249	4.40965	4.54368	4.69913	4.88244	5.10316	5.37614	5.72590	6.19639
	(b) Second natural frequency								
0	22.0345	22.2540	22.5018	22.7860	23.1186	23.5193	24.0211	24.6873	25.6558
	22.0345[a]	–	–	22.7860[a]	–	–	24.0211[a]	–	25.6558[a]
0.1	21.3381	21.5503	21.7898	22.0645	22.3864	22.7741	23.2602	23.9062	24.8471
0.2	20.6210	20.8256	21.0567	21.3220	21.6327	22.0074	22.4774	23.1028	24.0153
0.3	19.8806	20.0776	20.3001	20.5555	20.8550	21.2163	21.6699	22.2741	23.1578
	19.8806[a]	–	–	20.5555[a]	–	–	21.6699[a]	–	23.1578[a]
0.4	19.1138	19.3029	19.5166	19.7620	38.4920	20.3975	20.8343	21.4170	22.2710
0.5	18.3173	18.4982	18.7029	18.9381	19.2141	19.5476	19.9671	20.5276	21.3513
0.6	17.4879	17.6604	17.8557	18.0803	18.3441	18.6631	19.0649	19.6026	20.3952
	17.4879[a]	–	–	18.0803[a]	–	–	19.0649[a]	–	20.3952[a]
0.7	16.6253	16.7891	16.9746	17.1881	17.4392	17.7433	18.1268	18.6412	19.4021
0.8	15.7427	15.8972	16.0725	16.2744	16.5123	16.8009	17.1657	17.6564	18.3855
	(c) Third natural frequency								
0	61.6972	61.9096	62.1525	62.4361	62.7763	63.1992	63.7515	64.5266	65.7470
	61.6972[a]	–	–	62.4361[a]	–	–	63.7515[a]	–	65.7470[a]
0.1	58.9799	59.1886	59.4269	59.7046	60.0369	60.4489	60.9854	61.7364	62.9156
0.2	56.1923	56.3970	56.6303	56.9017	57.2257	57.6264	58.1466	58.8725	60.0094
0.3	53.3222	53.5226	53.7506	54.0152	54.3304	54.7192	55.2224	55.9224	57.0157
	53.3222[a]	–	–	54.0152[a]	–	–	55.2224[a]	–	57.0157[a]
0.4	50.3537	50.5492	50.7714	51.0288	51.3346	51.7108	52.1963	52.8693	53.9173
0.5	47.2648	47.4550	47.6708	47.9203	48.2161	48.5789	49.0456	49.6904	50.6914
0.6	44.0248	44.2090	44.4175	44.6583	44.9432	45.2916	45.7384	46.3534	47.3051
	44.0248[a]	–	–	44.6583[a]	–	–	45.7384[a]	–	47.3051[a]
0.7	40.5879	40.7650	40.9654	41.1964	41.4691	41.8018	42.2270	42.8104	43.7103
0.8	36.8846	37.0532	37.2439	37.4635	37.7223	38.0375	38.4392	38.9886	39.8336
	(d) Fourth natural frequency								
0	120.902	121.115	121.360	121.648	121.997	122.438	123.025	123.873	125.264
	120.902[a]	–	–	121.648[a]	–	–	123.025[a]	–	125.264[a]
0.1	115.187	115.398	115.639	115.922	116.264	116.693	117.264	118.083	119.422
0.2	109.318	109.526	109.763	110.040	110.374	110.792	111.345	112.135	113.421
0.3	103.267	103.471	103.704	103.975	104.301	104.707	105.241	106.001	107.231
	103.267[a]	–	–	103.975[a]	–	–	105.241[a]	–	107.231[a]
0.4	96.9954	97.1956	97.4234	97.6883	98.005	98.3982	98.9130	99.6419	100.815
0.5	90.4505	90.6462	90.8685	91.1261	91.4332	91.8128	92.3072	93.0031	94.1166
0.6	83.5541	83.7446	83.9605	84.2101	84.5064	84.8712	85.3438	86.0050	87.0561
	83.5541[a]	–	–	84.2101[a]	–	–	85.3438[a]	–	87.0561[a]
0.7	76.1821	76.3664	76.5747	76.8149	77.0992	77.4477	77.8967	78.5208	79.5059
0.8	68.1164	68.2928	68.4918	68.7209	68.9911	69.3210	69.7438	70.3275	71.2418

Table 3 Continued

c_h	c_b 0	0.1	0.2	0.3	0.4	0.5	0.6	0.7	0.8
	(e) Fifth natural frequency								
0	199.86	200.073	200.319	200.609	200.963	201.414	202.023	202.917	204.426
	199.86[a]	–	–	200.609[a]	–	–	202.022[a]	–	204.426[a]
0.1	190.146	190.357	190.599	190.885	191.232	191.672	192.262	193.126	194.574
0.2	180.163	180.372	180.611	180.891	181.23	181.659	182.231	183.062	184.448
0.3	169.862	170.067	170.303	170.577	170.909	171.324	171.877	172.675	173.998
	169.862[a]	–	–	170.577[a]	–	–	171.877[a]	–	173.998[a]
0.4	159.173	159.376	159.606	159.875	160.198	160.6	161.133	161.897	163.154
0.5	148.002	148.2	148.426	148.688	149.001	149.39	149.901	150.629	151.817
0.6	136.203	136.397	136.617	136.871	137.174	137.548	138.035	138.725	139.842
	136.203[a]	–	–	136.871[a]	–	–	138.035[a]	–	139.842[a]
0.7	123.543	123.732	123.944	124.189	124.48	124.838	125.301	125.95	126.991
0.8	109.594	109.774	109.978	110.212	110.489	110.828	111.263	111.868	112.828
	(f) Sixth natural frequency								
0	298.556	298.769	299.015	299.307	299.664	300.122	300.745	301.673	303.268
	298.556[a]	–	–	299.307[a]	–	–	300.745[a]	–	303.268[a]
0.1	283.842	284.054	284.297	284.584	284.935	285.381	285.986	286.88	288.408
0.2	268.716	268.926	269.166	269.448	269.791	270.226	270.811	271.671	273.131
0.3	253.099	253.306	253.543	253.820	254.155	254.577	255.142	255.967	257.357
	253.099[a]	–	–	253.820[a]	–	–	255.142[a]	–	257.357[a]
0.4	236.886	237.089	237.322	237.593	237.919	238.328	238.872	239.660	240.978
0.5	219.924	220.124	220.352	220.616	220.933	221.328	221.850	222.600	223.842
0.6	201.986	202.182	202.404	202.661	202.968	203.347	203.845	204.555	205.719
	201.986[a]	–	–	202.661[a]	–	–	203.845[a]	–	205.719[a]
0.7	182.698	182.888	183.104	183.352	183.647	184.010	184.482	185.149	186.230
0.8	161.360	161.543	161.750	161.988	162.269	162.613	163.056	163.676	164.668
	(g) Seventh natural frequency								
0	416.983	417.204	417.451	417.744	418.103	418.566	419.200	420.153	421.813
	416.991[a]	–	–	417.744[a]	–	–	419.200[a]	–	421.813[a]
0.1	396.278	396.490	396.734	397.022	397.375	397.826	398.441	399.358	400.947
0.2	374.979	375.189	375.430	375.714	376.059	376.498	377.093	377.974	379.490
0.3	352.982	353.190	353.428	353.706	354.043	354.470	355.044	355.888	357.329
	352.982[a]	–	–	353.706[a]	–	–	355.044[a]	–	357.329[a]
0.4	330.136	330.341	330.574	330.847	331.175	331.589	332.141	332.947	334.311
0.5	306.221	306.423	306.650	306.918	307.238	307.637	308.166	308.932	310.216
0.6	280.910	281.108	281.332	281.591	281.900	282.284	282.789	283.512	284.712
	280.911[a]	–	–	281.591[a]	–	–	282.789[a]	–	284.712[a]
0.7	253.658	253.851	254.068	254.318	254.616	254.983	255.461	256.140	257.251
0.8	223.436	223.621	223.830	224.07	224.354	224.701	225.151	225.781	226.796
	(h) Eight natural frequency								
0	555.115	555.379	555.626	555.919	556.280	556.747	557.389	558.360	560.073
	555.115[a]	–	–	559.919[a]	–	–	557.389[a]	–	560.073[a]
0.1	527.453	527.665	527.909	528.199	528.553	529.008	529.630	530.565	532.203
0.2	498.952	499.162	499.404	499.688	500.035	500.478	501.080	501.977	503.538
0.3	469.511	469.720	469.958	470.237	470.576	471.006	471.586	472.446	473.927
	469.511[a]	–	–	470.237[a]	–	–	471.587[a]	–	473.927[a]
0.4	438.925	439.130	439.365	439.638	439.969	440.386	440.944	441.763	443.163
0.5	406.897	407.099	407.329	407.597	407.918	408.321	408.855	409.634	410.949
0.6	372.980	373.179	373.404	373.664	373.975	374.362	374.872	375.606	376.833
	372.980[a]	–	–	373.671[a]	–	–	374.872[a]	–	376.841[a]
0.7	336.431	336.624	336.842	337.095	337.394	337.764	338.248	338.936	340.070
0.8	295.831	296.018	296.228	296.470	296.756	297.107	297.559	298.197	299.236

[a] Results of Downs [10]

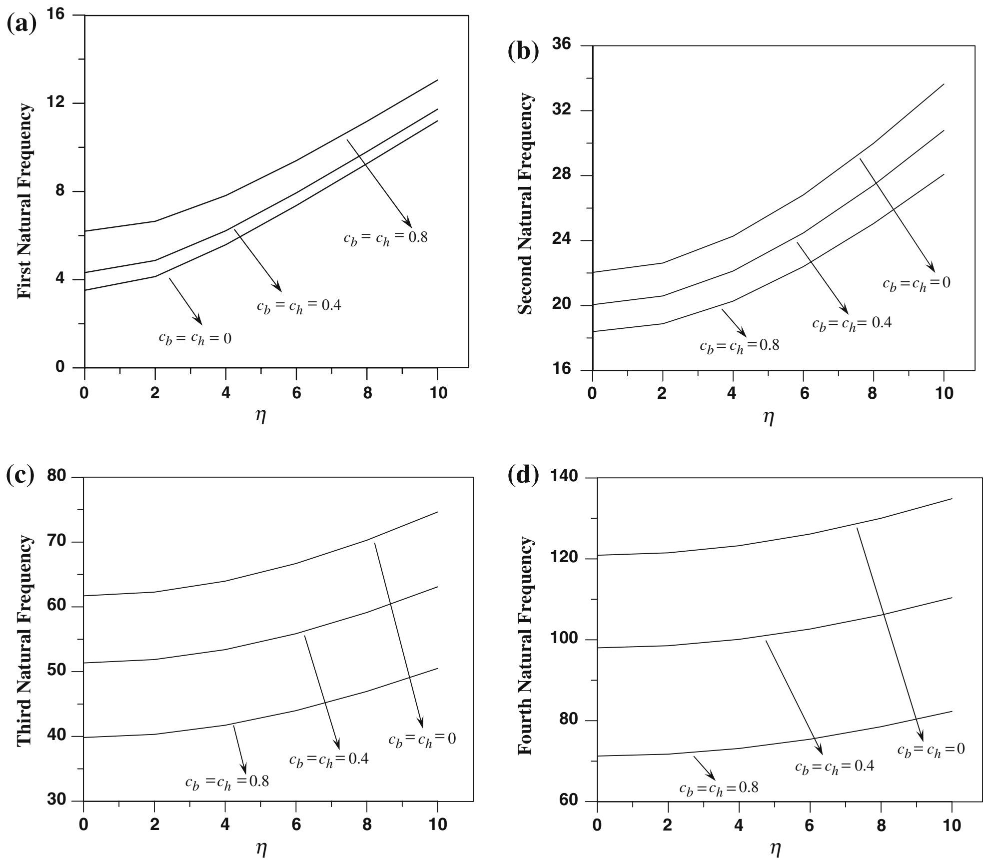

Fig. 2 Variation of the (**a**) first (**b**) second (**c**) third (**d**) fourth natural frequency with respect to the rotational speed parameter, η and taper ratios, c_b and c_h. ($\delta = 0$)

4 Formulation with DTM

In the solution step, the differential transform method is applied to Eq. (12) by using the theorems introduced in Table 1 and the following analytical expression is obtained.

$$\begin{aligned}
&\left[\frac{c_b c_h}{4}(k+1)(k-2)\eta^2 - c_b c_h \mu^2\right] W[k-2] \\
&+ \left[\frac{1}{3}(-c_b - c_h + c_b c_h \delta)\eta^2 (k-1)(k+1) + (c_b + c_h)\mu^2\right] W[k-1] \\
&+ \left[c_b c_h^3 (k-1) k (k+1)(k+2) + \frac{1}{2}(-c_b\delta - c_h\delta + 1) k (k+1)\eta^2 - \mu^2\right] W[k] \\
&+ \left[-c_h^2 (3c_b + c_h)(k-2)(k-1) k (k+1) + (k+1)^2 \delta \eta^2\right] W[k+1] \qquad (19) \\
&+ \left\{3c_h (c_b + c_h)(k+1)^2 (k+2)^2 + \eta^2 (k+1)(k+2)\left[\frac{1}{2}(-1 + c_b\delta + c_h\delta) + \frac{1}{3}(c_b + c_h - c_b c_h \delta) - \left(\frac{1}{4}c_b c_h + \delta\right)\right]\right\} W[k+2] \\
&- \left[(k+1)(k+2)^2 (k+3)(c_b + 3c_h)\right] W[k+3] \\
&+ (k+1)(k+2)(k+3)(k+4) W[k+4] = 0.
\end{aligned}$$

Additionally, the differential transform method is applied to Eqs. (13) and (14) at $x_0 = 0$ by using the theorems introduced in Table 2 and the following transformed boundary conditions are obtained.

$$W[0] = W[1] = 0 \quad \text{at } \xi = 0 \qquad (20)$$

Table 4 Variation of the first four natural frequency parameters, μ with respect to the rotational speed parameter, η, and the hub radius parameter, δ ($c_b = 0, c_h = 0.5$)

Natural Frequency Parameters								
η	$\delta = 0$				$\delta = 2$			
1	3.98662	18.474	47.4173	90.6039	4.38668	18.8795	47.8308	91.0305
	3.98662[a]	18.474[a]	47.417[a]	–	4.38668[a]	18.8795[a]	47.8308[a]	–
	3.9866[b]	18.474[b]	47.417[b]	–	–	–	–	–
2	4.4368	18.9366	47.8716	91.0626	5.74259	20.473	49.4867	92.7467
	4.4368[a]	18.9366[a]	47.8716[a]	–	5.7426[a]	20.473[a]	49.4866[a]	–
	4.4368[b]	18.937[b]	47.872[b]	–	–	–	–	–
3	5.09267	19.6839	48.619	91.8216	7.45274	22.8795	52.1206	95.5314
	5.09268[a]	19.6839[a]	48.6189[a]	–	7.45275[a]	22.8795[a]	52.1205[a]	–
	5.0927[b]	19.684[b]	48.619[b]	–	–	–	–	–
4	5.87876	20.6852	49.6456	92.873	9.31032	25.8663	55.5817	99.2847
	5.87796[a]	20.685[a]	49.6456[a]	–	9.31032[a]	25.8662[a]	55.5816[a]	–
	5.8788[b]	20.685[b]	49.646[b]	–	–	–	–	–
η	$\delta = 0.5$				$\delta = 1$			
1	4.09041	18.5762	47.521	90.7108	4.19156	18.6779	47.6245	90.8175
2	4.79784	19.3325	48.281	91.4869	5.1328	19.7202	48.6865	91.9090
3	5.77735	20.5311	49.520	92.7647	6.38678	21.3437	50.4034	93.6972
4	6.90501	22.0996	51.2013	94.5221	7.79308	23.4255	52.7063	96.1394

[a] Özdemir and Kaya [1]
[b] Hodges and Rutkowski [11]

$$\sum_{k=2}^{\infty} k(k-1)W\left[k\right] = \sum_{k=3}^{\infty} k(k-1)(k-2)$$
$$W\left[k\right] = 0 \quad \text{at } \xi = 1 \tag{21}$$

In Eqs. (19)–(21), $W\left[k\right]$ is the differential transform of $\tilde{w}(\xi)$. Using Eq. (19), $W\left[k\right]$ values for $k = 4, 5\ldots$ can now be evaluated in terms of c_b, c_h, μ, η, d_2 and d_3. These values, achieved by using the Mathematica computer package for $\delta = 0$, are as follows

$$\begin{aligned}
W[2] =& \ d_2 \\
W[3] =& \ d_3 \\
W[4] =& \ \frac{1}{2}(c_b + 3c_h)\, d_3 - \frac{1}{144}\Big\{ \\
& 72c_h^2 - 6\eta^2 + 4\eta^2 c_h \\
& + c_b\left[4\eta^2 - 3c_h\left(\eta^2 - 24\right)\right]\Big\} d_2 \\
W[5] =& \ \frac{1}{120}\Big\{ 12\, c_h^2 (3c_b + c_h)\, d_2 \\
& - \Big[108c_h^2 + (2c_h - 3)\,\eta^2 \\
& + \frac{1}{2}(c_b + 3c_h)\Big[\Big(-72c_h^2 + 6\eta^2 - 4c_h\eta^2 \\
& - 4c_b\eta^2 - 72c_hc_b + 3c_hc_b\eta^2\Big) d_2 \\
& + (216c_h + 72c_b)\, d_3\Big]\Big]\Big\}
\end{aligned}$$

The coefficients are obtained to numerical accuracy and the constants d_2 and d_3 that appear in $W\left[k\right]$'s are given by

$$d_2 = W[2] = \frac{1}{2!}\left(\frac{\mathrm{d}^2\tilde{w}}{\mathrm{d}\xi^2}\right)_{x=0},$$
$$d_3 = W[3] = \frac{1}{3!}\left(\frac{\mathrm{d}^3\tilde{w}}{\mathrm{d}\xi^3}\right)_{x=0} \tag{22}$$

5 Results and discussions

The computer package Mathematica is used to write a computer code for the expressions obtained using DTM. In order to validate the calculated results, comparisons with the studies in open literature are made and related graphics are plotted. The effects of the taper ratios, c_b and c_h, the rotational speed parameter, η and the hub radius parameter, δ, are investigated and the calculated results

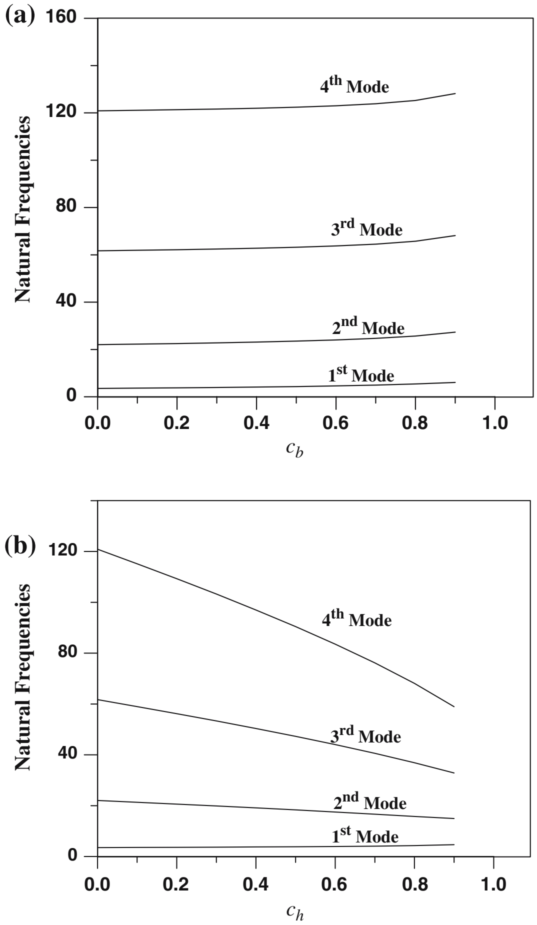

Fig. 3 Effect of the (**a**) breadth taper ratio, c_b (**b**) the height taper ratio, c_h, on the first four natural frequencies. ($\delta = 0$; $\eta = 0$)

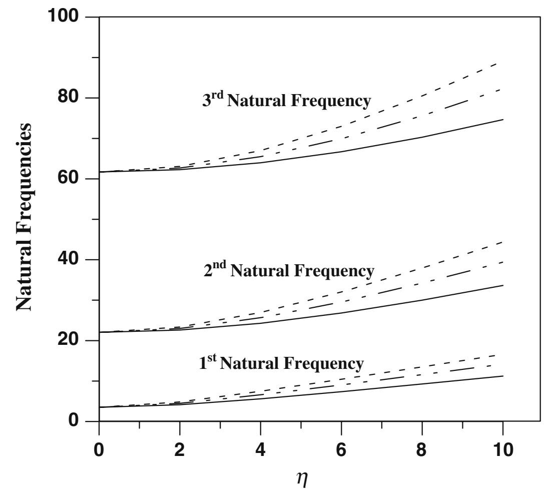

Fig. 4 Variation of the first three natural frequencies with respect to the hub radius parameter, δ and the rotational speed parameter, η ($\delta = 1$, ----; $\delta = 0.5$, –. . –; $\delta = 0$, —)

that can be used as reference values for the future studies are tabulated in several tables and figures.

In Table 3a–h, variation of the first eight natural frequencies of a nonrotating Euler–Bernoulli beam with different combinations of breadth and height taper ratios is introduced and the results are compared with the ones in the study of Downs [10] and as it is seen in these tables, there is a very good agreement between the results.

In Fig. 2a–d, variation of the first four natural frequencies with respect to both the taper ratios and the rotational speed parameter is introduced. Here both of the taper ratios have the same value. As it is observed in Figs. 2a–d, the rotational speed parameter has an increasing effect on the natural frequencies at every taper ratio because the centrifugal force that is proportional to the rotational speed has a stiffening effect that increases the natural frequencies. Additionally, when the Figs. 2a–d are examined, it is seen that the taper ratios have an increasing effect on the fundamental natural frequency while they have an decreasing effect on the other natural frequencies.

Moreover, in order to observe the effects of the taper ratios seperately, Fig. 3a–b can be considered. As it is seen in these figures, the breadth taper ratio, c_b, has very little, even no influence on the flapwise bending frequencies while the height taper ratio, c_h, has a linear decreasing effect on the natural frequencies except the fundamental natural frequency.

The rotational speed parameter, η, and the hub radius parameter, δ have significant effects on the values of the natural frequencies as it is introduced in Table 4. These results are compared with the ones in Özdemir and Kaya [1] and Hodges and Rutkowski [11]. The values of the natural frequency parameter, μ, increase as the rotational speed parameter, η, increases and the rate of increase becomes larger with the increasing hub radius parameter,δ because the centrifugal force is directly proportional to both of these parameters as it can be seen in Eq. (2). For a better insight and also in order to establish the trend, these effects are shown in Fig. 4 where the first three natural frequencies are plotted for three different values of the hub radius parameter and for several values of the rotational speed parameter.

6 Conclusion

A new and semi-analytical technique called the differential transform method is applied to the problem of a rotating double tapered Euler–Bernoulli beam in a simple and accurate way and the natural frequencies are calculated and the related graphics are plotted. The effects of the hub radius, taper ratios and rotational speed are investigated. The numerical results indicate that the flextural natural frequencies increase with the rotational speed and hub radius while they decrease with the height taper ratio. The calculated results are compared with the ones in literature and great agreement is considered.

References

1. Özdemir Ö, Kaya MO (2006) Flapwise bending vibration analysis of a rotating tapered cantilevered Bernoulli–Euler beam by differential transform method. J Sound and Vib 289:413–420
2. Zhou JK (1986) Differential transformation and its application for electrical circuits. Huazhong University Press, PR, China
3. Chiou JS, Tzeng JR (1996) Application of the Taylor transform to nonlinear vibration problems. Trans Am Soc Mech Eng J Vib Acoust 118:83–87
4. Jang MJ, Chen CL, Liu YC (2001) Two-dimensional differential transform for partial differential equations. Appl Mathe Comput 121:261–270
5. Abdel IH, Hassan H (2002) On solving some eigenvalue-problems by using a differential transformation. Appl Math Comput 127:1–22
6. Chen CK, Ju SP (2004) Application of differential transformation to transient advective–dispersive transport equation. Appl Math Comput 155:25–38
7. Arikoglu A, Ozkol I (2005) Solution of boundary value problems for integro-differential equations by using differential transform method. Appl Math Comput 168(2):1145–1158
8. Bert CW, Zeng H (2004) Analysis of axial vibration of compound bars by differential transformation method. J Sound Vib 275:641–647
9. Banerjee JR (2001) Dynamic stiffness formulation and free vibration analysis of centrifugally stiffened Timoshenko beams. J Sound Vib 247(1):97–115
10. Downs B (1977) Transverse vibrations of cantilever beam having unequal breadth and depth tapers. J Appl Mech 44:737–742
11. Hodges DH, Rutkowski MJ (1981) Free vibration analysis of rotating beams by a variable order finite element method. Am Instit Aeronaut Astronaut J 19:1459–1466